ADD

Interaction Notes

Note 405

March 1981

Characterization of Source Region EMP Penetration Through a Hatch Aperture

F.C. Yang

The Dikewood Corporation
Santa Monica, California 90405

Abstract

The source region EMP penetration through the hatch aperture at one end of a flanged cylinder is analyzed. The penetration is characterized by the open circuit voltage induced across the hatch gap. Quasi-static approximation is used. The results are presented by simple circuit diagrams.

Acknowledgement

The author would like to thank Drs. K.S.H. Lee and K.F. Casey and Mr. C. Jones of Dikewood for helpful suggestions.

CONTENTS

ILLUSTRATIONS

I. INTRODUCTION

The access hatch of a flanged cylinder (Figure 1), although preventing the equipment inside the cylinder from direct exposure to EMP and radiation, allows EMP penetration through the hatch rim. This report will characterize such EMP penetration in a source region.

In the following section frequency-domain results will first be derived. Then, the time-domain results will be discussed. In deriving the results quasi-static approximations will be used throughout, so that the effects due to the electric field, magnetic field and Compton current can be considered separately.

II. FORMULATION AND RESULTS

Under the quasi-static limit, the electromagnetic fields penetrated into the cylinder shown in Figure 1 due to an incident electric field, magnetic field and Compton current can be considered separately. Each of these incident sources creates a nonzero tangential electric field at the hatch aperture (or, in other words, generates a nonzero voltage across the gap), which, in turn, acts as the source for equipment inside the cylinder. In this section, equations and equivalent circuit diagrams for calculating the tangential electric field will first be constructed in the frequency domain. Then, the appropriate techniques of Laplace transformations and convolution integrations will be used to calculate the time-domain quantities.

1. FREQUENCY-DOMAIN FORMULATION

a. Incident Electric Field

Instead of considering the geometry of Figure 2 directly, the simplified geometry of Figure 3 will be studied. The results from the simplified study can be modified to obtain the results for the original geometry (Fig. 2).

For the problem depicted in Figure 3, the tangential electric field $\tilde{\vec{E}}^{I}_{a}$ at the aperture A due to an incident electric field $\tilde{\vec{E}}^{inc}$ can be calculated by solving the following integro-differential equation

$$-2\hat{z}\cdot\nabla\times\iint_{A}\left[s\varepsilon_1 G_1(\vec{r},\vec{r}') + s\varepsilon_o G_o(\vec{r},\vec{r}')\right](\hat{z}\times\tilde{\vec{E}}^{I}_{a})dS' = 2s\varepsilon_1\hat{z}\cdot\tilde{\vec{E}}^{inc}, \quad \vec{r} \text{ in } A \qquad (1)$$

where

$$G_i = \frac{e^{-s\sqrt{\mu_o\varepsilon_i}\,|\vec{r}-\vec{r}'|}}{4\pi|\vec{r}-\vec{r}'|}, \quad i = 0,1$$

ε_1 (= $\varepsilon_o + \sigma/s$) and ε_o are, respectively, the permittivities of the regions above and below $z = 0$.

Under the quasi-static approximation $\left(|s\sqrt{\mu_o\varepsilon_i}\,b| << 1\right)$, and the condition that the gap width of the aperture w is much smaller than the hatch radius b, one can apply Taylor's expansion to the exponential

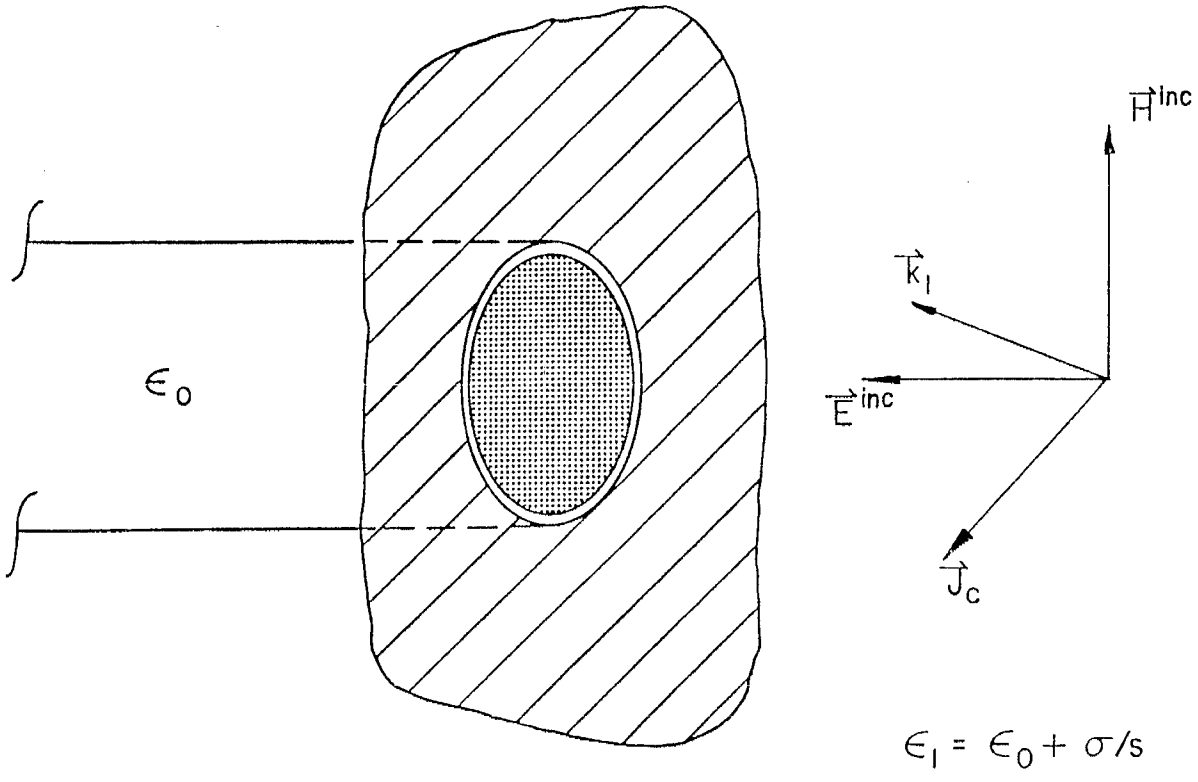

Figure 1. Model for a cylinder in the source region environment.

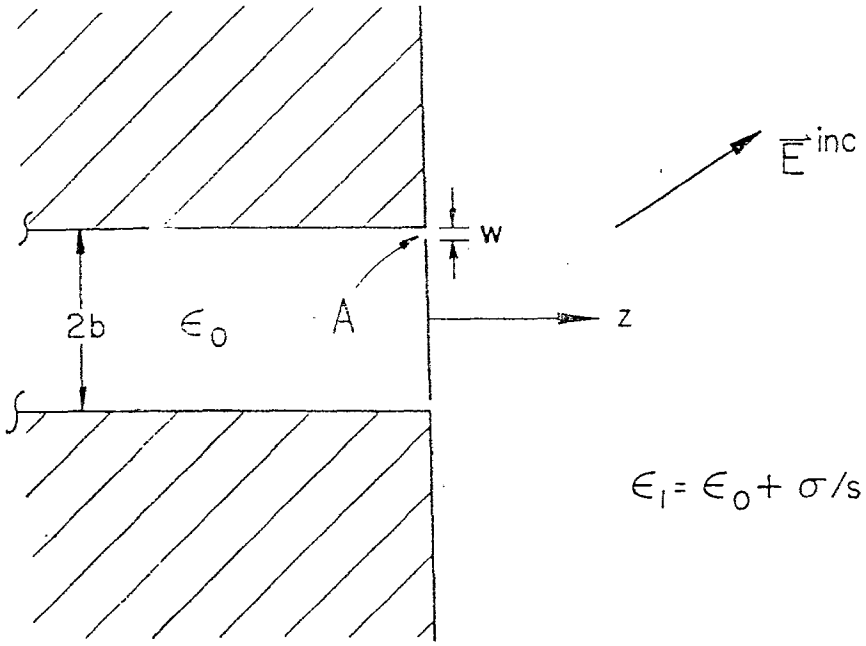

SIDE VIEW

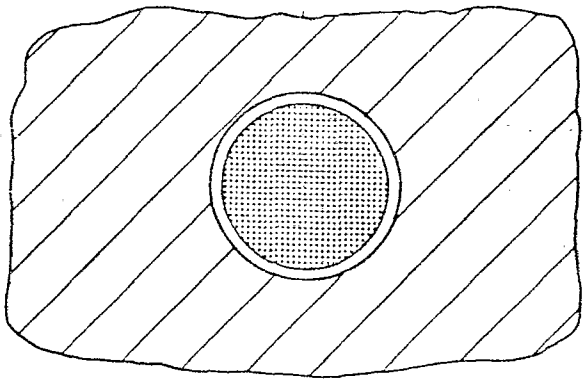

FRONT VIEW

Figure 2. The configuration of a flanged cylinder with a hatch aperture on one end exposed to a source region electric field.

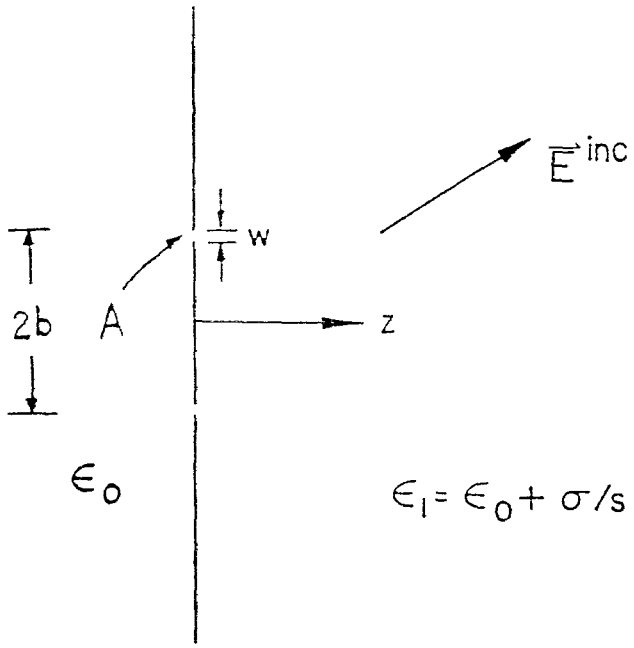

SIDE VIEW

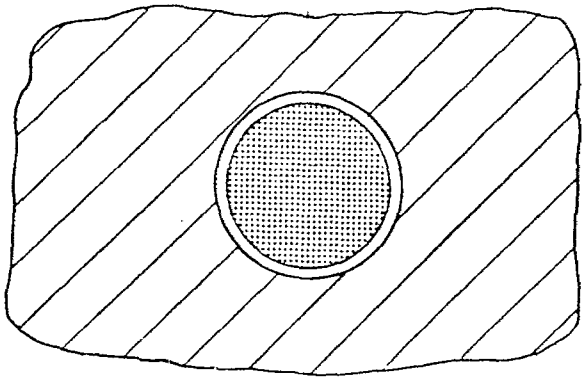

FRONT VIEW

Figure 3. An infinite plate with a hatch aperture exposed to a source region electric field.

functions in G_1 and then uses asymptotic antenna theory to reduce Equation 1 to the following form:

$$-(s\varepsilon_o + s\varepsilon_1)\frac{\tilde{E}^I_{aw}}{\pi b}\Omega = 2s\varepsilon_1\tilde{E}^{inc}_z \tag{2}$$

where

$$\Omega = 2[\ell n(32b/w) - 2] \tag{3}$$

$$\tilde{\vec{E}}^I_a = \hat{\rho}\,\tilde{E}^I_a \tag{4}$$

Equation 2 can be rearranged as

$$\tilde{V}^I = \tilde{E}^I_a w = -\frac{2\pi b^2 s\varepsilon_1 \tilde{E}^{inc}_z}{2\Omega s\varepsilon_o b + \Omega\sigma b} \tag{5}$$

which can be represented by a simple circuit diagram pictured in Figure 4a with

$$\tilde{I}^I_{sc} = -s\varepsilon_1\pi b^2\tilde{E}^{sc} \qquad (\tilde{E}^{sc} = 2\,\tilde{E}^{inc}_z)$$

$$C_1 = \varepsilon_o\Omega b \tag{6}$$

$$R_1 = (\Omega\sigma b)^{-1}$$

The circuit in Figure 4a is for the aperture field of Figure 3. For the more realistic geometry of Figure 2, the circuit has to be modified. Intuitively, the modified circuit can be drawn as Figure 4b. In the modified circuit, C_2 is one-half of the capacitance between the circular disc and the circular cylinder depicted in Figure 5. The evaluation of C_2 has been given in detail in Reference 1 and is estimated at

$$C_2 = 4\varepsilon_o b\ \ell n[(16b/w) - 2] \tag{7}$$

The circuit in Figure 4b is for an unloaded hatch aperture. When the aperture is loaded with an impedance, the appropriate circuit for the loaded

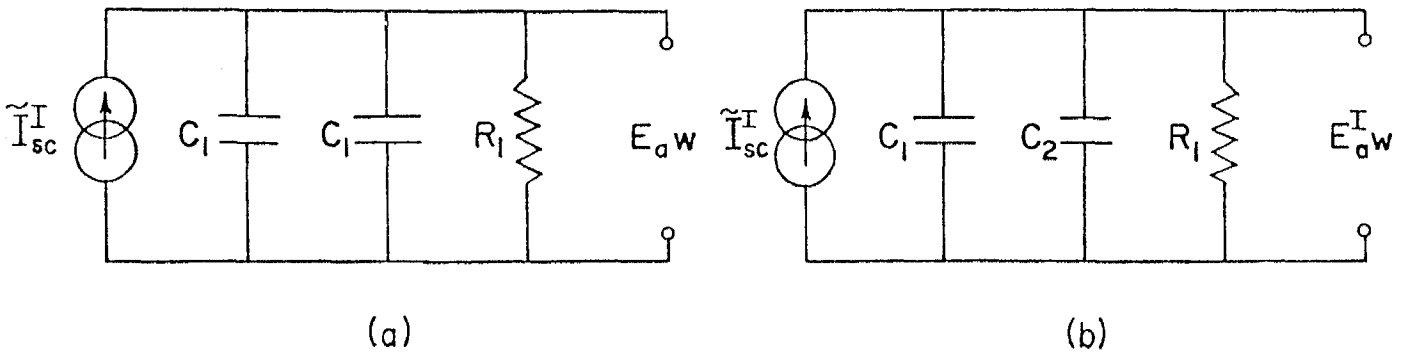

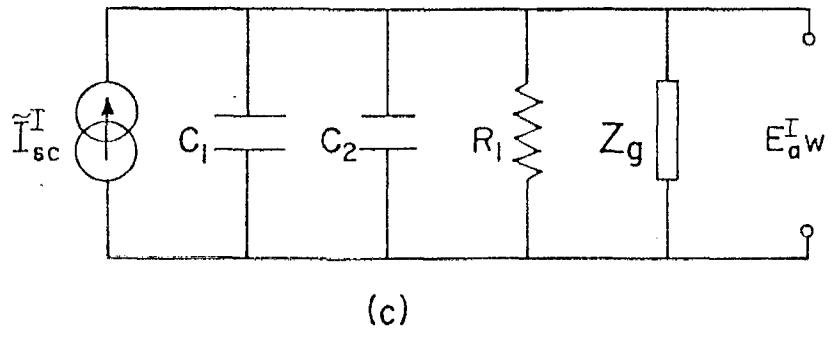

$$\tilde{I}^I_{sc} = -s\epsilon_1 \pi b^2 \tilde{E}^{sc}$$

$$C_1 = \epsilon_0 \Omega b \,, \quad C_2 = \epsilon_0 \Omega' b$$

$$R_1 = (\Omega \sigma b)^{-1}$$

$$\Omega = 2\left[\ln(32\, b/w) - 2\right]$$

$$\Omega' = 4\left[\ln(16\, b/w) - 2\right]$$

Z_g = gasket impedance

Figure 4. The open-circuit voltage induced across the hatch aperture of (a) Figure 3, (b) Figure 2, (c) Figure 2 with gasket impedance, due to a source region electric field.

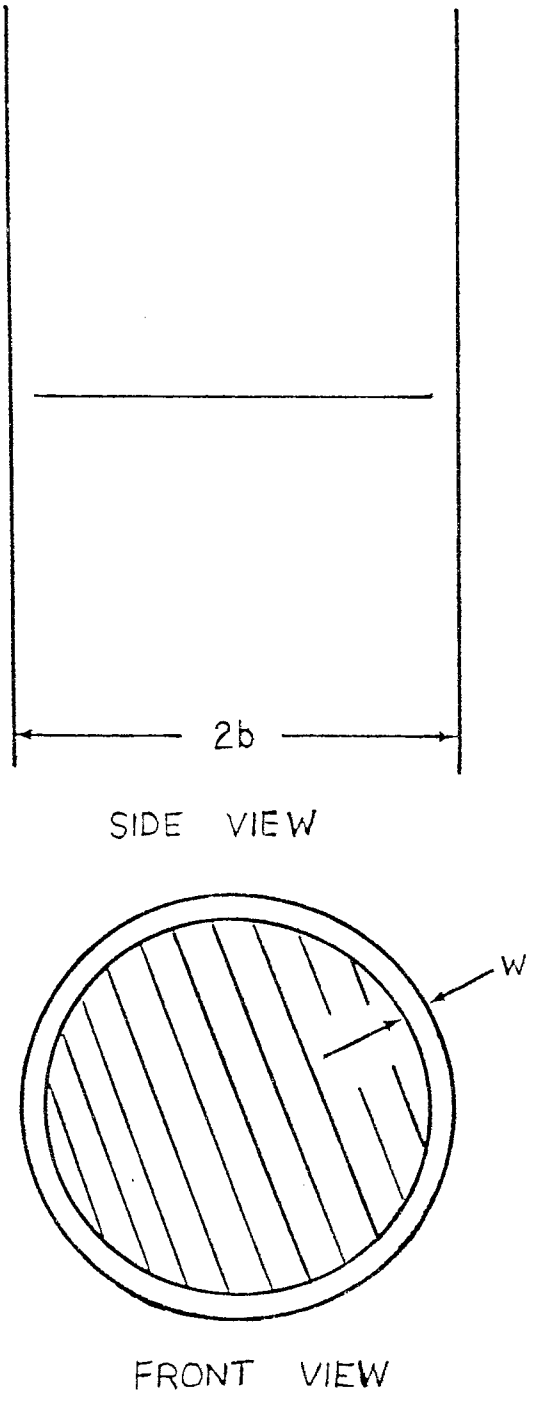

Figure 5. A circular disc inside a circular cylinder.

aperture is, from physical reasoning, drawn in Figure 4c (Ref. 2). In the figure, Z_g is the gasket impedance. From the circuit, the aperture voltage due to an incident electric field is

$$\tilde{V}^I = \tilde{E}_a^I w = \frac{\tilde{I}_{sc}}{s(C_1 + C_2) + 1/R_1 + 1/Z_g} \tag{8}$$

b. Incident Magnetic Field

As far as the aperture field excited by an incident magnetic field $\tilde{\vec{H}}^{inc}$ is concerned, the problem of Figure 6a can be approximated by that of Figure 6b. In Figure 6b, the tangential electric field $\tilde{\vec{E}}_a^{II}$ at the aperture can be calculated by solving the following integro-differential equation

$$-2\int\int_A \left[s\varepsilon_1 \vec{\vec{\Gamma}}_1(\vec{r},\vec{r}') + s\varepsilon_o \vec{\vec{\Gamma}}_o(\vec{r},\vec{r}')\right] \cdot (\hat{z} \times \tilde{\vec{E}}_a^{II}) dS' = -2\hat{z} \times (\hat{z} \times \tilde{\vec{H}}^{inc}), \quad \vec{r} \text{ in } A \tag{9}$$

where

$$\vec{\vec{\Gamma}}_i(\vec{r},\vec{r}') = \left(\vec{\vec{I}} - \frac{1}{s^2 \mu_o \varepsilon_i} \nabla_t \nabla_t\right) G_i(\vec{r},\vec{r}')$$

Equation 9 can be solved by using the same approximation as that for the incident electric field case to obtain the following formula

$$-\frac{\tilde{E}_a^{II} w\Omega}{2\pi} \cos\phi \left[\sigma\left(1 + \frac{1}{s\mu_o \sigma b^2}\right) + \frac{1}{s\mu_o b^2}\right] \simeq \tilde{H}^{sc} \cos\phi \tag{10}$$

where

$$-2\hat{z} \times (\hat{z} \times \tilde{\vec{H}}^{inc}) = \hat{y}\, \tilde{H}^{sc}$$

$$\tilde{\vec{E}}_a^{II} = \hat{\rho}\, \tilde{E}_a^{II} \cos\phi \tag{11}$$

Equation 10 is rewritten as

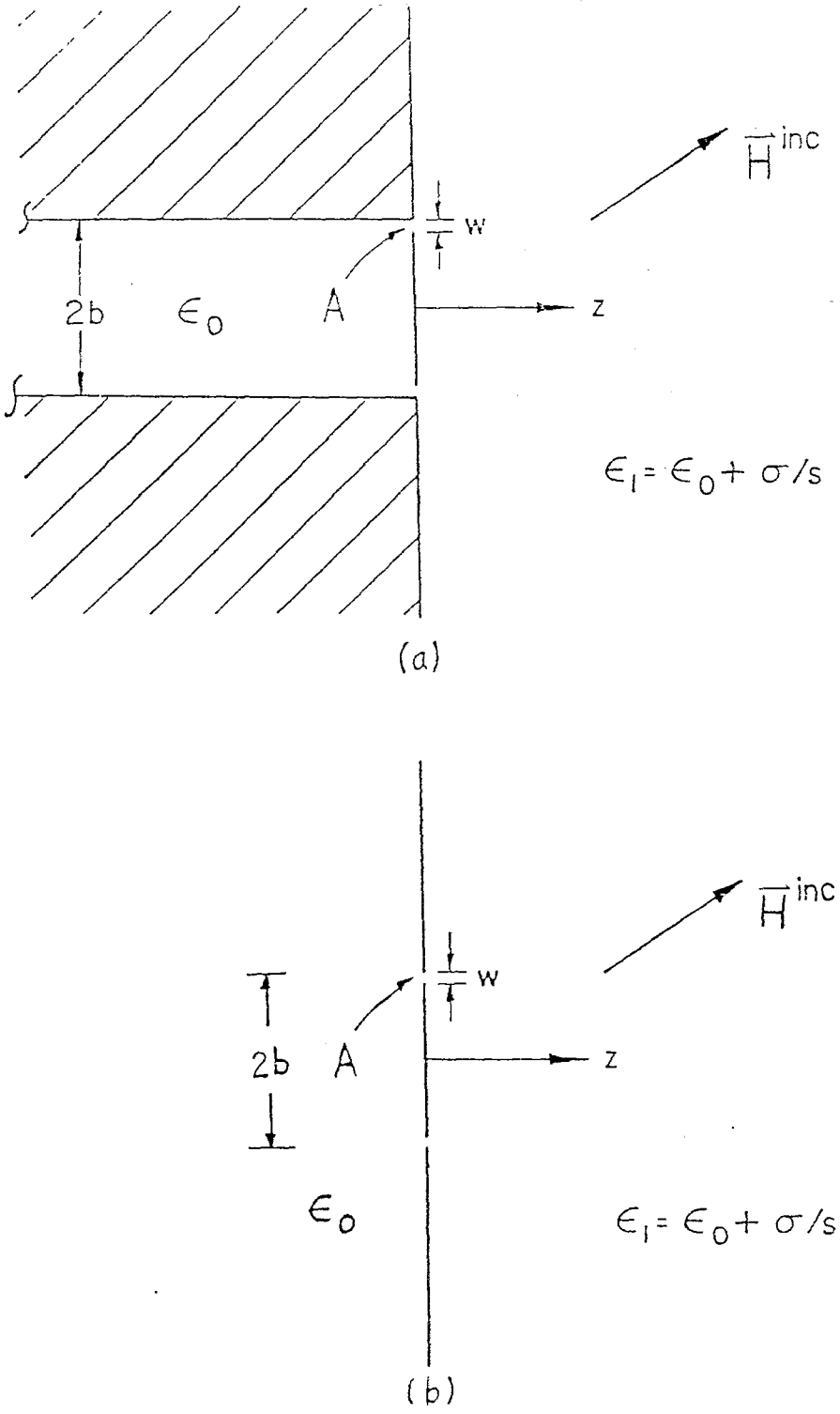

Figure 6. (a) A flanged cylinder with a hatch aperture on one end exposed to a source region magnetic field, and, (b) an infinite plate with a hatch aperture exposed to a source region magnetic field.

$$\tilde{V}^{II} = \tilde{E}_a^{II}{}_w = - \frac{\pi b \tilde{H}^{sc}}{\Omega/(s\mu_o b) + \Omega\sigma b/2}$$

$$= \frac{\tilde{I}_{sc}^{II}}{1/(sL_2) + 1/R_2} \qquad (12)$$

which can be represented by a simple circuit diagram (see Figure 7a) with

$$\tilde{I}_{sc}^{II} = - \pi b \tilde{H}^{sc}$$

$$L_2 = \mu_o b/\Omega \qquad (13)$$

$$R_2 = 2/(\Omega\sigma b)$$

A similar argument as that for the incident electric field case can also be used to obtain the circuit diagram for a loaded aperture excited by a magnetic field (also, see Ref. 2). The circuit diagram is shown in Figure 7b. From the circuit, the voltage across the loaded gap due to an incident magnetic field is simply

$$\tilde{V}^{II} = \tilde{E}_a^{II}{}_w = \tilde{I}_{sc}^{II} / \left(\frac{1}{sL_2} + \frac{1}{R_2} + \frac{1}{Z_g} \right) \qquad (14)$$

An alternative circuit depicted in Figure 7c can also be used.

c. Compton Current

If one considers the effect of the incident electric field, in the incident electric field case (i.e., 1a), as depositing charges onto the hatch, the circuit diagram given in Figure 4 becomes self-explanatory. Since the Compton current has the same effect of depositing charges onto the hatch, the aperture field $\tilde{E}_a^{III}$ can be calculated with a similar circuit diagram. The required circuit diagram is shown in Figure 8. The corresponding equation for $\tilde{E}_a^{III}{}_w$ (or, $\tilde{V}^{III}$) will be similar to Equation 8, i.e.,

$$\tilde{V}^{III} = \tilde{E}_a^{III}{}_w = \tilde{I}_{sc}^{III} / [s(C_1 + C_2) + 1/R_1 + 1/Z_g] \qquad (15)$$

In Figure 8 and Equation 15 the current source $\tilde{I}_{sc}^{III}$ is given as follows:

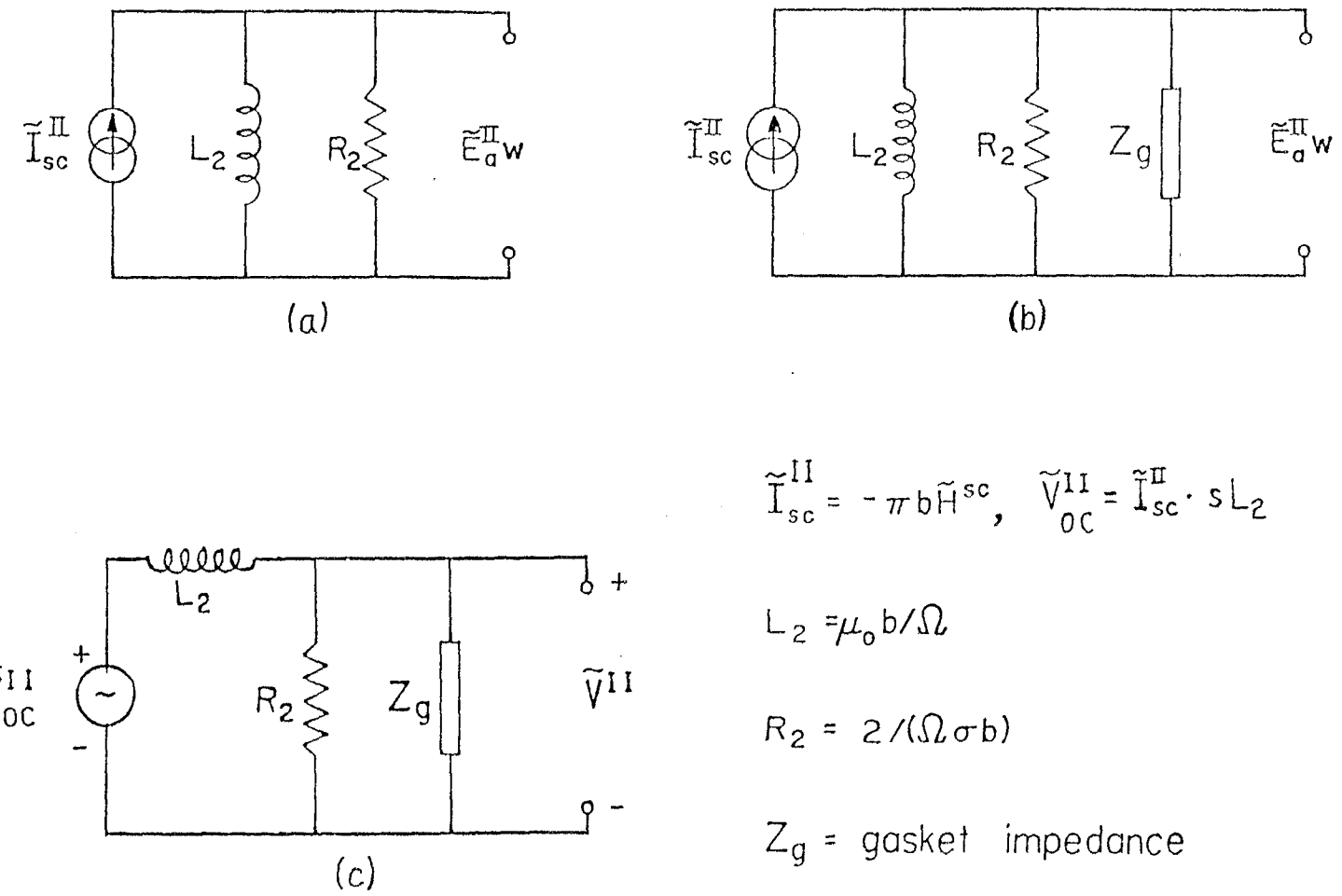

Figure 7. The open-circuit voltage induced across the hatch aperture of Figure 6 due to a source region magnetic field, (a) without gasket impedance, (b) with gasket impedance, and, (c) the Thévenin equivalent of (b).

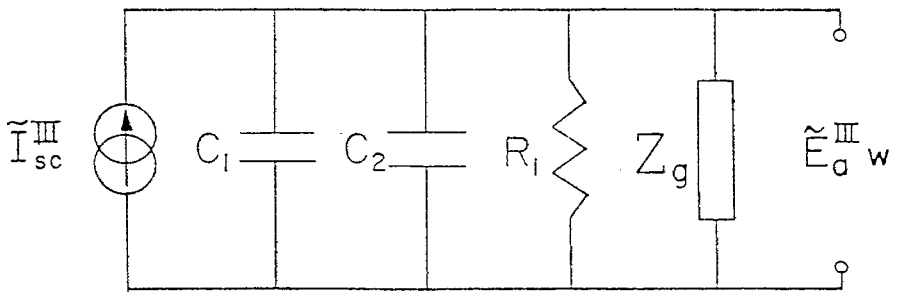

$$\tilde{I}^{III}_{sc} = \tilde{J}_c \cdot M / m\gamma \,, \qquad \text{if Gamma thin}$$

$$= \tilde{J}_c \cdot \pi b^2 \,, \qquad \text{if Gamma thick}$$

$$C_1 = \epsilon_0 \, \Omega \, b \,, \qquad C_2 = \epsilon_0 \, \Omega' b$$

$$R_1 = (\Omega \sigma b)^{-1} \,, \qquad Z_g = \text{gasket impedance}$$

$$\Omega = 2 \left[\ln(32\, b/w) - 2 \right]$$

$$\Omega' = 4 \left[\ln(16\, b/w) - 2 \right]$$

Figure 8. The open-circuit voltage induced across the impedance loaded hatch aperture of a flanged cylinder due to a source region Compton current.

If the hatch door is Gamma thin, then

$$\tilde{I}_{sc}^{III} = \tilde{J}_c(\text{Amp/m}^2)\cdot M(\text{Kg})/m_\gamma(\text{Kg/m}^2) \tag{16}$$

where $\tilde{J}_c$ is the Compton current density, M and m_γ are the mass and energy absorption mass of the hatch door.

If the hatch door is Gamma thick, then

$$\tilde{I}_{sc}^{III} = \tilde{J}_c(\text{Amp/m}^2)\cdot S(\text{m}^2) \tag{17}$$

where $S = \pi b^2$ is the cross-sectional area of the hatch.

2. TIME-DOMAIN RESULTS

The convolution integrations will be used to calculate the time-domain results. Before carrying out the convolution integrations, one has to know the necessary impulse responses. The impulse responses for the sources of an electric field, magnetic field and Compton current can be obtained by calculating the inverse Laplace transforms of Equations 8, 14 and 15 with $\tilde{I}_{sc}^{i}$, i = I, II, III set equal to 1. That is, one has the impulse response $h^{I,III}(t)$ for an electric field or Compton current source given by

$$h^{I,III}(t) = (C_1 + C_2)^{-1} e^{-t/\tau_e} u(t) \tag{18}$$

and the impulse response $h^{II}(t)$ for a magnetic field source given by

$$h^{II}(t) = (1/R_2 + 1/Z_g)^{-1}[\delta(t) - \tau_m^{-1} e^{-t/\tau_m} u(t)] \tag{19}$$

where

$$\tau_e = (C_1 + C_2)R_1 Z_g/(R_1 + Z_g)$$

$$\tau_m = L_2(R_2 + Z_g)/(R_2 Z_g) \tag{20}$$

Once the impulse responses are known, the time-domain results for the sources $I_{sc}^{i}(t)$, i = I, II, III are simply given by

$$V^i(t) = wE_a^i(t) = \int_0^t I_{sc}^i(t')h^i(t-t')dt' \qquad (21)$$

REFERENCES

1. Sneddon, I.N., Mixed Boundary Value Problems in Potential Theory, North-Holland Publishing Company, Amsterdam, 1966.

2. Lee, K.S.H., editor, "EMP Interaction: Principles, Techniques and Reference Data," EMP Interaction 2-1, Air Force Weapons Laboratory, Kirtland AFB, NM, December 1980.